ON-LINE BIREFRINGENCE MEASUREMENT IN FILM BLOWING PROCESS

Hiroshi Ito [(a)], Ken-ichi Suzuki [(a)], Takeshi Kikutani [(a)] Ho-Jong Kang [(b)], Toshitaka Kanai [(c)]
(a) Dep.of Organic and Polym.Materials, Tokyo Institute of Technology, JAPAN
(b) Dept. of Polym. Sci. and Eng., Dankook University, KOREA
(c) Plastics Tech. Center, Idemitsu Petrochemical Co., Ltd., JAPAN

Abstract

On-line measurements of velocity, bubble diameter, temperature and three principal birefringences were performed during the tubular film extrusion of polypropylene at various draw ratios and blow-up ratios. Birefringence increased rapidly in the vicinity of the frost line height where the crystallization started. Birefringence between MD and ND showed the maximum value near the solidification position, and then it decreased with increasing distance from the die, and eventually the obtained PP film showed almost uniaxial molecular orientation.

Introduction

Film blowing process is one of the most important film formation processes in the industry. The film blowing is a complex process involving interaction between fluid rheology, heat transfer and free surface kinematics. Formation of high-order structure such as molecular orientation and crystallization also proceeds during the process. There are several publications that discuss kinematics, dynamics and structure formation of film blowing from the measurements of the deformation rate, drawing force and pressure inside the bubble [1-18]. In particular, it is important to analyze the mechanism of structure development in the process because ultimate film properties are governed by the high-order structure. In terms of the on-line measurements of structure development, several researchers carried out the on-line optical retardation measurement [3, 15-17] and laser Raman spectroscopy [18]. Since the films show uni- and bi-axial molecular orientation in blowing process, we need to analyze the three principal birefringences**,** which are defined from three refractive indices (n_{MD}, n_{TD} and n_{ND}). However, there are few reports in which the on-line measurement of three principle birefringences is applied to film blowing process.

Recently, we started the on-line measurements of optical retardation using a laser light source with a rotating polarizing filter, and analyzed the birefringence development in high-speed melt spinning process and film drawing process [19-21]. To evaluate the three principal birefringences in film drawing, we conducted the on-line birefringence measurement directing the laser beam from two different angles. In this study, in order to clarify the mechanism of structure development in film blowing process, we measured the velocity, bubble diameter, temperature, inside pressure and optical retardation in the blowing process of polypropylene.

Experimental

Materials and Tubular Film Extrusion

Homo-polypropylene (PP) resin (Idemitsu Petrochemical Co., Ltd, F-704NP, MFR=7) was used in this study. A 50 mm single screw extruder (PLACO, LL50C) with a circular film-blowing die (outer diameter = 100 mm and die gap at exit = 2 mm) was used. To apply quenching air to the film surface, an air-ring of 100 mm thick was set immediately above the die. The extrusion was carried out at a temperature of 195 ^{o}C and a polymer flow rate of about 20.4 kg/h. The draw ratios (= take-up velocity / extrusion velocity at die exit; DRs) of 29 and 42 and blow-up ratios (= final bubble diameter / die diameter; BURs) of 2.5 and 2.8 were adopted.

On-line Measurements

Axial velocity of film was measured by a standard tracer technique and used to determine strain rates in the machine direction (MD). The thickness profiles were calculated from the velocity and bubble diameter profiles using the mass balance equation. Temperature measurements along the length of the bubble were carried out using an infrared pyrometer (NEC san-ei Instruments, TH5104). A contact-type thermometer (RTc, DP-300) was also used for the region where the film was solidified. Pressure inside the bubble was measured by a H_2O manometer and used to determine the stress in the transverse direction (TD).

Figure 1 shows a typical photograph of tubular film and the optical retardation measuring system consisting of a He-Ne laser light source, a rotating polarizing filter, a photo detector etc. [19-21]. The laser light source and the photo detector were arranged horizontally so that laser-beam paths through the two identical points of the bubble before reaching the photo detector. The distance from the die and the incident angle to the film surface was changed shifting the position of the set of laser light source and photo detector vertically and horizontally as shown in the figure.

In principle, three refractive indices (n_{MD}, n_{TD} and n_{ND}) and three principal birefringences ($\Delta n_{MD\text{-}TD}$, $\Delta n_{MD\text{-}ND}$ and $\Delta n_{TD\text{-}ND}$) can be determined from the two retardations measured at two different angles, the mean refractive index and the thickness of film. In this experiment, a set of horizontal incident angles θ=0^{o} and 20^{o} or θ=0^{o} and 30^{o} were selected. The angle

θ corresponds to the rotation of incident beam with respect to the MD axis. On the other hand, additional rotation of the incident beam with respect to the TD axis was taken into account for the analysis of the region where the bubble was inflated.

Results and discussion

Variations of bubble diameter and axial film velocity along the length of the bubble are shown in Figure 2. The regions where the frost line (FL) was observed are also indicated in the figure. The position of FL was around 22 cm at DR 42 with BUR 2.5 and DR 29 with BUR 2.8, whereas it was around 24 cm at DR 29 and BUR 2.5. Change of the bubble diameter continued up to the FL. On the other hand, the velocity profiles showed a tendency of saturation 2 - 5 cm below the FL. The thickness profiles calculated from these results using the mass balance equation are shown in Figure 3. The thickness decreased along the length of bubble and became constant above the FL. The strain rates in the MD and TD directions were calculated from the bubble diameter and axial velocity. Both strain rates showed maximum values near the air-ring and decreased to zero above the FL. The maximum strain rate was higher at higher DR and the peak for TD strain rate shifted to the downstream at high BUR.

Figure 4 shows the temperature profiles of bubble surface at several blowing conditions. In general, film temperature decreased along the length of bubble due to cooling by the quenching air. After initial rapid decrease of temperature, however, the film started to crystallize in the vicinity of the FL thereby causing a plateau in the temperature profile. The temperature started to decrease again above 30 cm because of the reduction of crystallization rate and decreased asymptotically to ambient temperature. The temperatures at the plateau were about 90 ^{o}C, and were independent of film blowing conditions.

Figure 5 shows the results of the optical retardation measurements at three different incident angles. The retardations were low in the melt zone and increased drastically in the vicinity of the FL. The retardations also increased with an increase of incident angles. The change of birefringence $\Delta n_{MD\text{-}TD}$ along the bubble length is shown in Figure 6. In the region where the bubble diameter was increasing, the birefringence was analyzed from the retardations measured at $\theta=0^{o}$ and 20^{o} considering the inflation angle of the bubble. $\Delta n_{MD\text{-}TD}$ was also low in the melt zone before the FL. However, it increased rapidly near the FL where the crystallization started. Even after the solidification of film, which was confirmed from the constant thickness, $\Delta n_{MD\text{-}TD}$ continued to increase slightly. The $\Delta n_{MD\text{-}TD}$ of obtained film was higher at higher DR.

Figure 7 displays the changes of three principal birefringences along the bubble length at DR 29 and BUR 2.5. It was difficult to analyze the birefringences $\Delta n_{TD\text{-}ND}$ and $\Delta n_{MD\text{-}ND}$ properly in the vicinity of the FL because of a combination of the fluctuation of the position of FL and the steep increase of retardation in this region. It was confirmed, however that the $\Delta n_{MD\text{-}ND}$ reached a maximum value after the steep increase of retardation and decreased with increasing distance from the die. This result indicated that the film had planar orientation near the solidification position and then gradually changed to almost uniaxial orientation in the course of additional structural change after the solidification.

From the results for measured temperature (see Fig.4), we fitted and calculated the temperature using the energy equation without crystallization term [9]. From the between estimated and measured temperate profiles, the crystallization behavior was estimated at DR 29 and BUR 2.5. Figure 8 shows the in-plane birefringence $\Delta n_{MD\text{-}TD}$ as a function of crystallinity. The crystallization occurred at low birefringence around 0.0008, and this value was applicable stress-optical rule. The stress-optical coefficient (SOC) for PP is about 0.8GPa^{-1} [20], and the applicable stress means only 1MPa. This result indicated that critical birefringence value, which was gradually increase before crystallization, is almost same between film blowing and fiber spinning processes.

Conclusions

We carried out on-line measurements of velocity, bubble diameter, temperature and optical retardation during the tubular film extrusion of polypropylene (PP) at various draw ratios (DRs) and blow-up ratios (BURs). To evaluate three principal birefringences, the measurement of retardation was also conducted by directing the laser beam from two different angles with respect to the film surface. Birefringence was low in the melt zone and increased rapidly in the vicinity of the frost line (FL) where the crystallization started. Even after the solidification of film, $\Delta n_{MD\text{-}TD}$ continued to increase slightly. $\Delta n_{MD\text{-}ND}$ showed a maximum value near the solidification position indicating the tendency of planar orientation, and then decreased with increasing distance from the die. Finally the obtained PP film showed almost uniaxial molecular orientation in these experimental conditions.

Acknowledgment

This work was partially supported by the program of the Japan Society for the Promotion of Science (JSPS), a core university program between Tokyo Institute of Technology and Korean Advanced Institute of Science and Technology. This work also was partly supported by the Grand-in-Aid from the Ministry of Education, Science, Sports and Culture, Japan.

References

1. T.Kanai and G.A.Campbell, Film Processing, Progress in Polym.Process. Series, Hanser Publisher
2. J.R.A. Pearson and C.J.S. Petrie, J. Fluid Mech., **40**, 1-19 (1970)

3. T.Nagasawa, T.Matsumura and S.Hoshio, Appl.Polym.Symp., **20**, 275-293 (1973)
4. R.Farber and J.M.Dealy, Polym.Eng.Sci., **14**, 435 (1974)
5. C.D.Han and J.Y. Park, J.Appl.Polym.Sci., **19**, 3257-3276 (1975)
6. M.H.Wagner, Kunststoffe, **68**, 15-17 (1978)
7. R.K.Gupta, A.B.Metzner and K.F. Wissbrun, Polym.Eng.Sci., **22**, 172-181 (1982)
8. H.H.Winter, Pure&Appl.Chem., **55**, 943-976 (1983)
9. T.Kanai and J.L.White, Polym.Eng.Sci., **24**, 1185-1201 (1984)
10. T.A.Huang and G.A.Campbell, Adv.Polym.Technol., **5**, 181-192 (1985)
11. T.A.Huang and G.A.Campbell, J.Plast.Film&Sheet., **2**, 30-39 (1986)
12. R.Patel, T.Butler, K.Walton and G.Knight, Polym.Eng.Sci., **34**, 1506-1514 (1992)
13. A.Gupta, D.M.Simpson and I.R.Harrison, J.Appl.Polm.Sci., **50**, 2085-2093 (1993)
14. W.Michaeli and G.Schmitz, ANTEC'95 Tech.Paper, 181-185 (1995)
15. A.Ghanen-Fard, P.J.Carreau and P.G.Lafleur, J.Plast.Film&Sheet., **12**, 68-86 (1996)
16. A.Ghanen-Fard, P.J.Carreau and P.G.Lafleur, Polym.Eng.Sci., **37**, 1148-1163 (1997)
17. A.Ghanen-Fard, P.J.Carreau and P.G.Lafleur, Int.Polym.Process., **12**, 136-146 (1997)
18. S.Cherukupalli, A.A.Ogale, L.K.Henrichsen and A.J.McHugh, Proc.of PPS-18, (2002)
19. T.Kikutani, K.Nakao, W.Takarada and H.Ito, Polym.Eng.Sci., **39**, 2349-2357 (1999)
20. H.Urabe, H.Ito, T.Kikutani and N.Okui, Seikei-Kakou, **12**, 729-735 (2000)
21. H.Ito, K.Suzuki, T.Kikutani and K.Nakayama, ANTEC 2000 Tech.Paper, 1715-1719 (2000)

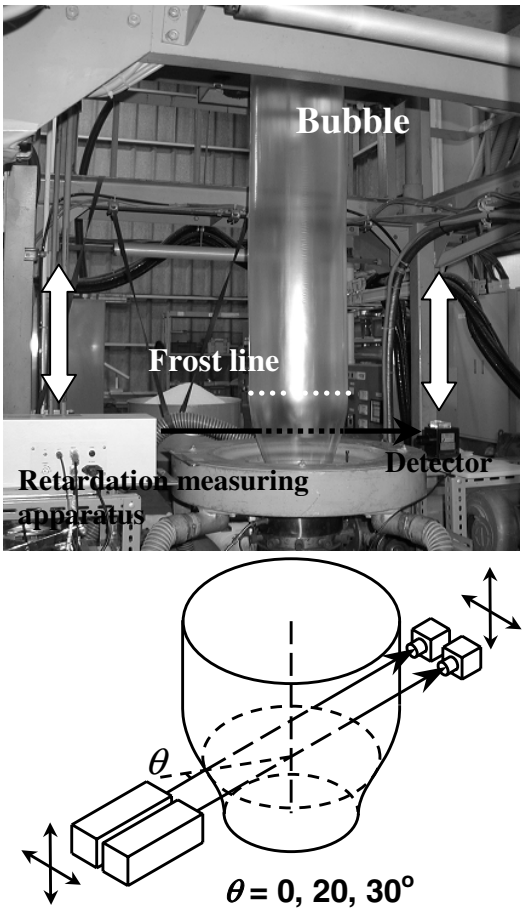

Figure 1 Schematic diagram of tubular film and optical retardation measuring system.

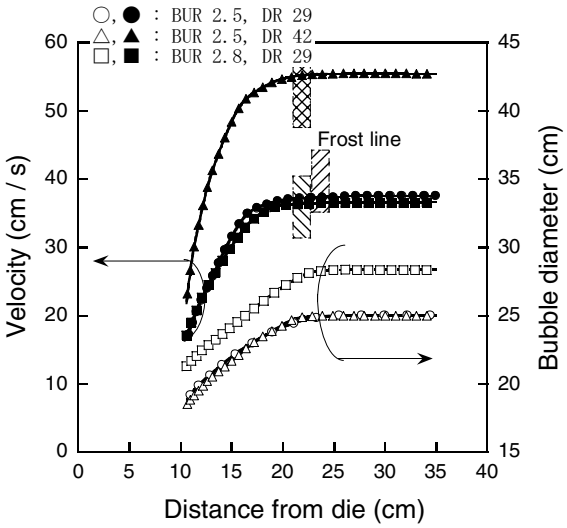

Figure 2 Velocity and diameter profiles of bubble at several blowing conditions.

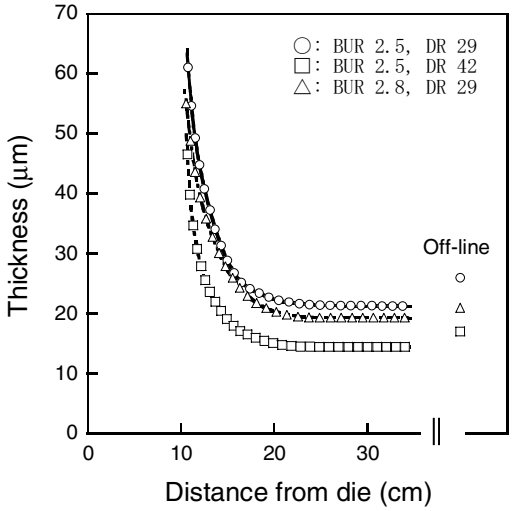

Figure 3 Thickness profiles of bubble at several blowing conditions.

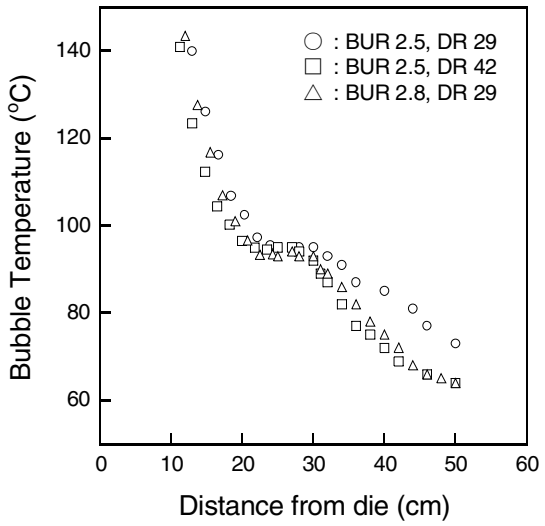

Figure 4 Temperature profiles of bubble surface at several blowing conditions.

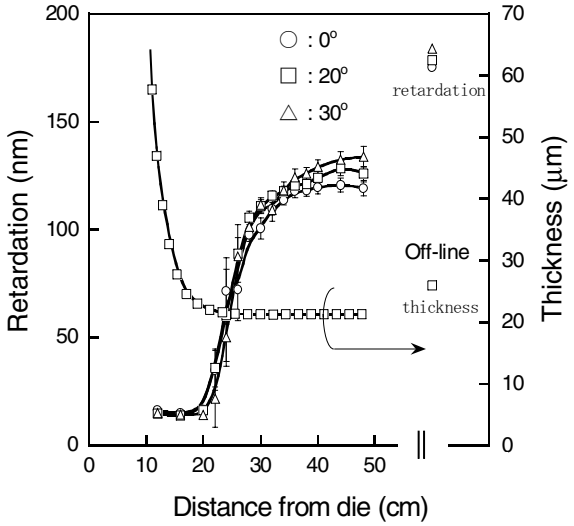

Figure 5 Retardation profiles at three different incident angles. DR and BUR were 29 and 2.5, respectively.

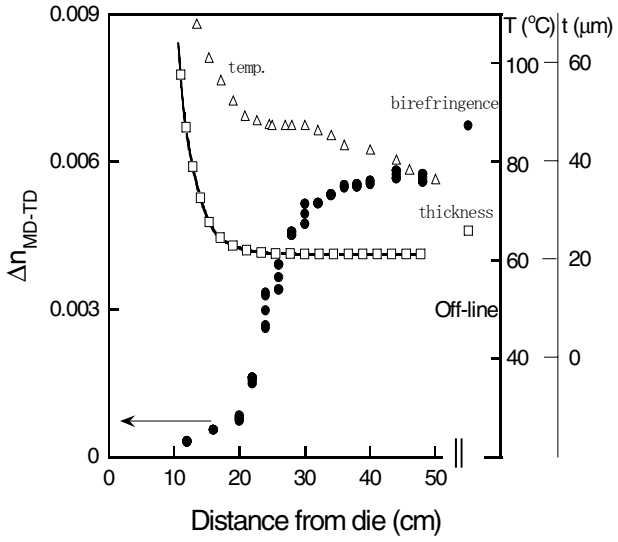

Figure 6 Birefringence $\Delta n_{MD\text{-}TD}$ profile at blowing condition of DR 29 and BUR 2.5.

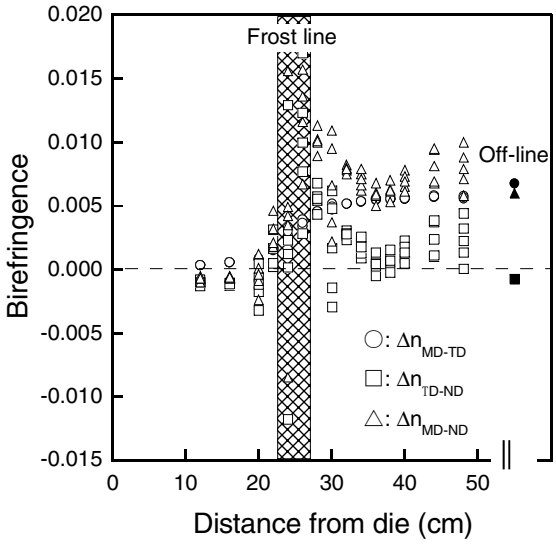

Figure 7 Profiles of three principal birefringence at blowing condition of DR 29 with BUR 2.5.

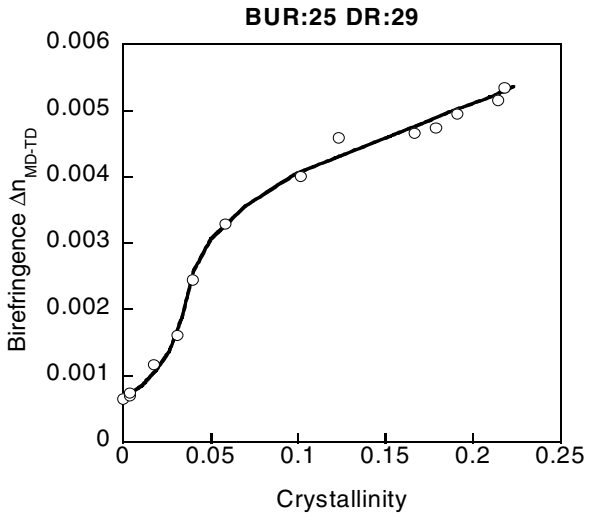

Figure 8 Birefringence as a function of estimated crystallinity at blowing condition of DR 29 with BUR 2.5.